DETECTION OF PROPAGATING WAVES THROUGHOUT THE CHROMOSPHERE IN NETWORK BRIGHT POINTS.

R. T. James M^{c}Ateer[1,*], Peter T. Gallagher[2,1], David R. Williams[3,1], Mihalis Mathioudakis[1], Kenneth J. H. Phillips[4], and Francis P. Keenan[1]

[*]E-mail: j.mcateer@qub.ac.uk
[1]Department of Pure and Applied Physics, Queen's University Belfast, Belfast, BT7 1NN, Northern Ireland, U.K.
[2]L-3 Communications Analytics Corp., NASA Goddard Space Flight Center, Greenbelt, Maryland 20771, U.S.A.
[3]Mullard Space Science Laboratory, Holmbury St. Mary, Dorking, Surrey, RH5 6NT, U. K.
[4]Space Science Department, Rutherford Appleton Laboratory, Chilton, Didcot, OX11 0QX, U. K.

ABSTRACT

We analysed oscillations in individual Network Bright Points (NBPs) in Ca II K_3, Hα core, Mg I b_2, and Mg I $b_1 - 0.4$ Å giving us a range of heights from the upper to the lower chromosphere. Lightcurves, and hence power spectra, were created by isolating distinct regions of the NBP via a simple intensity thresholding technique. Using this technique, it was possible to identify peaks in the power spectra with particular spatial positions within the NBPs. This was extended into the time domain by means of wavelet analysis. We track the temporal evolution of power in particular frequency bands by creating power curves. These are then cross-correlated across all observed wavelengths to search for propagating waves.

In particular, long-period waves with periods of 4–15 minutes (1–4 mHz) were found in the central portion of each NBP, indicating that these waves are certainly not acoustic, but possibly due to magneto-acoustic or magneto-gravity wave modes. We note the possible existence of fast-mode MHD waves in the lower chromosphere, coupling and transferring power to higher-frequency slow-mode MHD waves in the upper chromosphere.

Key words: Oscillations; Chromosphere; Photosphere; MHD waves.

1. INTRODUCTION

The solar atmosphere from the photosphere to the chromosphere is permeated by kilogauss magnetic fields. Flux emerges in the supergranular internetwork and is transported to the cell boundaries to form the chromospheric network. Further migration along the network results in regions of strong magnetic fields at the junction of several supergranular cells. These regions are sometimes termed Network Bright Points (NBPs). They show up in emission in strong chromospheric lines and display a one-to-one correlation with the underlying photospheric magnetic field [1]. Whereas the internetwork contains oscillations which can be explained as acoustic waves, the network seems to contain frequencies lower than the acoustic cut-off [2].

The precise role these NBP oscillations play in chromospheric heating has been the topic of much discussion, but the theories can be divided into two main camps. The first theory suggests the existence of downward-propagating magneto-gravity waves [3,4], a more detailed discussion of which can be found in [5]. The second theory suggests the existence of upwardly propagating magnetohydrodynamic (MHD) waves [6]. Fast-mode MHD waves in the NBPs at frequencies above the fast-mode cut-off are formed by granular buffeting at the photosphere [7,8]. These propagate up through the NBP such that their velocity amplitude will increase due to density statification. When their velocity becomes comparable to the tube speed, they enter the non-linear region and mode-coupling can occur [9]. The mode-coupling preferentially occurs by fast-mode waves at freqeuncy ν, which will transfer most of their energy to slow-mode waves at frequency 2ν, although some energy will be left in waves at the original frequency [9]. The fast-mode waves hence transfer most of their power to slow-mode waves, which can then shock and heat the surrounding plasma [10].

In the present paper we examine the oscillatory behaviour of NBPs in three dimensions to test the second theory outlined above. First, NBP oscillations are studied in Ca II K_3 as a function of the radial position from the NBP centre. Oscillations at the very bright centre are then studied in time using wavelet analysis. Finally oscillations are studied throughout the chromosphere by means of cross-correlation across all wavelengths.

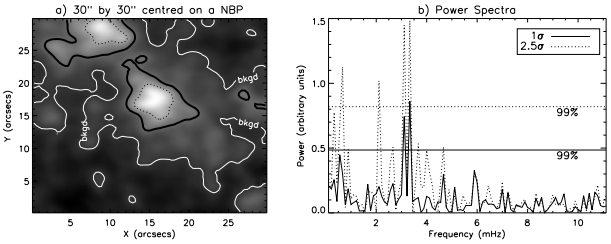

Figure 1. (a)- 30" × 30" time-averaged Ca II K_3 image of a sample NBP. The white line corresponds to the modal pixel value (the background). The solid and dashed lines correspond to contours at 1 and 2.5 standard deviations above the background respectively. Only pixels inside the closed contour around the central NBP are included. (b)- Fourier Transforms of the lightcurves resulting from the contours in (a). The corresponding 99% confidence levels for each FFT is also shown

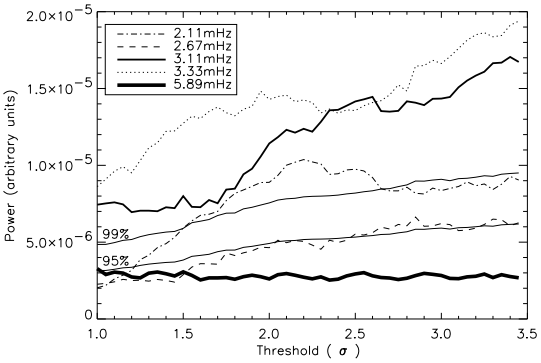

Figure 2. Oscillatory power against threshold (in standard deviations above the modal vlaue) for the NBP in Fig. 1. The 99% and 95% levles at each threshold are also shown

2. OBSERVATIONS

The observations were carried out on 1998 September 22, with the Richard B. Dunn Solar Telescope (DST) at the National Solar Observatory/Sacramento Peak and were taken as part of an eleven-day-long joint campaign with the *Transition Region And Coronal Explorer (TRACE)* spacecraft. The aim of the campaign was to examine the relationship between quiet sun events in the photosphere, chromosphere, and transition region. A 150 minute sequence of 100" × 100" images were obtained in Ca II K_3, Hα core, Mg I b_2, and Mg I $b_1 - 0.4$ Å, centred on a quiet sun field (Solar_X = -25", Solar_Y = -35") with a 45 s cadence. This provided several NBPs which could be clearly identified in all wavelengths. Co-alignment of the ground based images with the *TRACE* data led to a calculated resolution of 0.33" per pixel in the Ca II K_3 data and 0.18" per pixel for the other wavelengths. Analysis of the DST observations was carried out using standard routines within the *SolarSoftWare* package written in IDL. The data were corrected for CCD readout bias and flat-fielded. Each image was aligned to the first image of the series by means of cross-correlation.

3. RADIAL STUDY

For each NBP, the series of images were further divided into subfields of 30" × 30" centred on each point (Fig. 1). For each image in the series the NBP was contoured at a chosen threshold above the modal pixel value. The average pixel intensity inside the closed contour was calculated. This average NBP pixel intensity was combined with the background value (chosen as the modal pixel value) to create a contrast value for each image. The final lightcurve is then a series of contrast values [11]. The contour method ensures only pixels from inside the NBP are used [1,11] and the contrast lightcurve method removes any slowly varying trends from the data. Any remaining very low frequency power was further removed by digitally convolving the contrast curve with a suitable Bessel function.

Gradually increasing the chosen threshold of the contour, such that the bright centre of the NBP was increasingly isolated, provided a means of following the radial profile of any oscillations present. At high frequencies the power spectrum remained similar (Fig. 1b). However at low frequencies, it was found that peaks would suddenly appear, rapidly increase in power or even disappear altogether as the threshold was increased (Fig. 3). In each NBP different frequencies dominate [11], although there were a few common themes. The appearance of low frequencies often coincided with the disappearance of higher frequencies. This suggests that magnetism or gravity play a dominant role in NBPs at the expense of acoustic waves. Previous work [11] has shown how averaging over the entire network, or taking too small a sample of NBPs can lead to a lack of detection of all frequencies.

4. TEMPORAL STUDY

Wavelet analysis [12] was carried out on the lightcurves of maximum threshold (i.e. best isolation of the bright centre). An example wavelet power plot for Ca II K_3 is shown in Fig. 3. This clearly shows the transient nature of network oscillations, in the form of wave-packets at a specific frequency. The combination of wavelet analysis and Fourier tranforms is essential to ensure that these wave-packets are not missed, and that frequencies found are real. For a frequency peak to regarded as real, it was decided it must contain at least one full oscillation outside the cone of influence at greater than 95% confidence. A summary of these results can be found in [13].

5. PROPAGATING WAVES

'Power' curves were created by taking horizontal slices of the wavelet power transform [4] at each and every frequency (see Fig. 3d). For each wavelength pair, at each frequency, power curves were correlated and the maximum correlation and corresponding timelag recorded, hence creating a 3-D frequency-correlation-timelag curve. Maxima in the frequency-corrrelation

Table 1. Results from the NBP in Fig 1. Top- Oscillatory power in each wavelength in each frequency band. The 99 and 95 refer to the transform exceeding the 99% and 95% confidence levels respectively. Each of these frequencies existed in a wave-packet for at least one full oscillation in the wavelet transform. Bold numbers refer to wave-packets which existed for more than one full oscillation. Bottom- Correlation maxima across each wavelength pair. The range of values correspond to the frequency at peak correlation, ±0.1mHz. The final column denotes if the deduced speed is lower or higher than the acoustic velocity, C_s

	From:	1.00	1.33	1.67	2.00	2.33	2.67	3.00	3.33	3.67	4.00
λ	To:	1.22	1.56	1.89	2.22	2.56	2.89	3.22	3.56	3.89	4.22
Ca II K_3							95	**99**	**99**		**95**
Hα		**99,95**	**99**		95		99			**99**	**99,95**
Mg I b_2		99,99					99	95	95		
Mg I $b_1-0.4$ Å		99	**99,95**		99		95	99	95		

λ_1	λ_2	Correlation Factor	Frequency (mHz)	Timelag ($\times$ 45 seconds)	Vel. compared to c_s
Ca II K_3	Hα	0.66 – 0.79	1.2 – 1.4	-3 – -12	lower/higher
		0.61 – 0.72	2.3 – 2.5	4 – 6	lower/higher
Ca II K_3	Mg I b_2	0.68 – 0.75	1.9 – 2.1	0	higher
Ca II K_3	Mg I $b_1-0.4$ Å	0.57 – 0.62	1.73 – 1.93	3 – 7	lower/higher
Hα	Mg I b_2	0.77 – 0.84	1.2 – 1.4	-3 – -7	higher
Hα	Mg I $b_1-0.4$ Å	0.69	4.1 – 4.3	3	lower/higher
Mg I b_2	Mg I $b_1-0.4$ Å	0.69 – 0.79	1.5 – 1.7	0 – 3	lower/higher

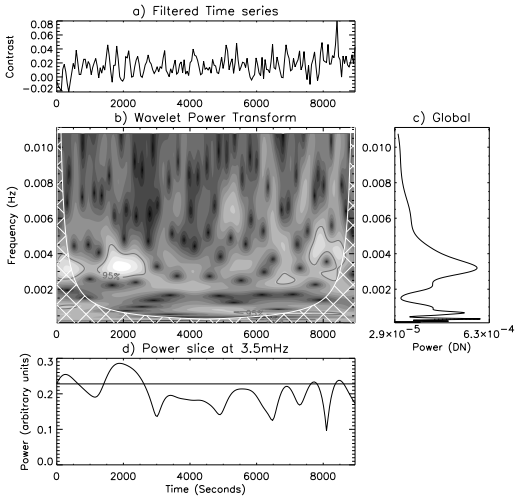

Figure 3. Wavelet transform of the maximum threshold Ca II K_3 lightcurve of the NBP in Fig 1.(a)- Filtered contrast curve. (b)- Wavelet power transfrom. Lighter areas indicate larger oscillatory power. The χ^2-derived 95% confidence level is also shown. The hatched area is the Cone Of Influence. Inside this area edge effects can affect the transform. (c)- Global wavelet power spectrum, analogous to a Fourier transform. (d)- Power curve at 3.5 mHz. A slice across the wavelet tranform in a 0.2 mHz band. The 95% significance level corresponding to the contours in b are also shown. The time axes of a,b and d are the same. The frequency axes of b and c are the same.

curve were selected, and retained only if the correlation factor was above 0.6, and the corresponding timelag was less than 450 sec (10 $\times$ 45 sec cadence). Correlations below 0.6 or with greater than 450 sec time lag were dismissed as false. The timelag value could then be combined with an estimate of height formation of each wavelength to produce a estimate of the velocity of the propagating wave [4,14]. For a data cadence of 45 sec (combined with uncertainty in the height of formation of each line) there are large errors in the deduced velocity values. Instead it was decided to calculate, for each wavelength pair, the minimum timelag corresponding to a wave travelling at the acoustic velocity, C_s ($\sim$ 9 km sec^{-1} in the chromosphere). A timelag greater than or equal to the acoustic velocity refers to a possible slow-mode MHD wave. A fast-mode wave will travel at a velocity greater than the Alfvén speed (minimum 30 km sec^{-1}), but with our limited velocity resolution we suggest that any wave with a velocity greater than C_s is a possible fast-mode wave.

The results from one NBP are shown in Table 1. The presence of a $\sim$1.9 mHz wave between Ca II K_3 and both Mg I b_2 and Mg I $b_1-0.4$ Å is clear (Mg I b_2 to Mg I $b_1-0.4$ Å also shows a correlation at a slightly lower frequency). The Fourier tranforms also show oscillatory power at $\sim$1.9 mHz in Mg I $b_1-0.4$ Å, which is reduced in Hα. There is a second peak at $\sim$4.0 mHz in Hα, which is reduced on reaching the Ca II K_3 level. Hα to Mg I $b_1-0.4$ Å shows a propagating wave at $\sim$4.1 mHz. This is consistent with the MHD theory of network heating[6]. A fast-mode wave at $\sim$1.9 mHz generated at the photosphere propagates up through the NBP at fast-mode speed. Around the height of Hα formation mode-coupling occurs, hence the onset of a $\sim$4.0 mHz oscillation, but with some remnant signal at $\sim$1.9 mHz. The slow-mode wave ($\sim$4.0 mHz) travels for a short time before shocking, thereby explaining the lack of this oscillation in Ca II K_3.

There is also some weak evidence for downward-moving waves. A $\sim$1.3 mHz correlation (Ca II K_3 to Hα and Hα to Mg I b_2) at slow-mode speed is found, although among these three wavelengths, an oscillatory signal at this frequency is found in Hα only. The $\sim$2.4 mHz correlation (Ca II K_3 to Hα) does not correspond to any wave-packet in either wavelength, and is therefore dismissed. This demonstrates the benefit of using wavelet analysis, as we can compare frequencies with wave-packets. There also seem to be many uncorrelated peaks in the 2.67–3.56 mHz range.

6. CONCLUSIONS

We have shown how NBP oscillations behave as a function of radial distance from the centre, as a function of time, as a function of height in the atmosphere. These are combined to show, for one NBP, evidence which supports the MHD theory of chromospheric heating in the network. An oscillation at a fast-mode frequency is seen to propagate upwards at a fast-mode speed to the upper chromosphere. Here it couples to a slow-mode wave at twice the original frequency. This slow-mode wave rapidly shocks in the upper chromosphere, although there is a remnant peak at the original fast-mode frequency. The quasi-periodic nature of these oscillations means that wavelet analysis is an ideal analysis tool. The lack of previous detection of these waves could be due to the fact that in ordinary Fourier transforms the wave-packets will be washed out by non-periodic components.

Further work will involve extending this study into the other NBPs in the field-of-view of our present data. Simulataneous TRACE data will also be used to study the transition region and corona. It is expected that mode-coupling, followed by slow-mode wave shocking, will mean there will be no correlation of the TRACE data with the ground-based data. A study of a larger number of NBPs, across more wavelengths and at higher cadence, will be neccessary to confirm these results. Simultaneous magnetograms will also be used to search for flux emergence coinciding with propagating wave-packets. A study over the entire lifetime of NBPs, from birth through to dissipation will show whether oscillations could be linked to underlying photospheric magnetic field strength.

ACKNOWLEDGMENTS

This work was supported by the U.K. Particle Physics and Astronomy Research Council and the Northern Ireland Department of Education and Learning. J MCA and DRW also thank QUB and RAL for CAST studentships. The DST observations were obtained by PTG as a visiting research student at the National Solar Observatory, National Optical Astronomy Observatories, operated by the Association of Universities for Research in Astronomy, Inc. (AURA), under cooperative agreement with the National Science Foundation. We also thank Dr. Tom Berger and Dr. Ray Smartt for useful advice and discussion regarding data analysis and acquisition. Wavelet software was provided by C. Torrence and G. Compo and is available at URL:http://paos.colorado.edu/research/wavelets/

REFERENCES

1. Cauzzi, G., Falchi, A., & Falciani, R. 2000, A&A, 357, 1090

2. Lites, B.W., Rutten, R.J. & Kalkofen, W. 1993, ApJ, 414, 345

3. Deubner, F.-L., & Fleck, B. 1990, A&A, 228, 506

4. Bocchialini, K., & Baudin, F. 1995, A&A, 299, 893

5. Lou, Y.-Q. 1995, MNRAS, 274, L1

6. Kalkofen, W. 1997, ApJ, 486, L145

7. Choudhuri,A.R., Auffret, H., & Priest E.R. 1993, Sol. Phys., 143, 49

8. Choudhuri,A.R., Dikpati, M., & Banerjee, D. 1993, 1993, Apj, 413, 811

9. Ulmschneider, P., Zähringer, K., & Musielak, Z.E. 1991, A&A, 241, 625

10. Zhugzhda, Y.D., Bromm V., & Ulmscheider P. 1995, A&A, 300, 302

11. M^{c}Ateer, R.T.J., Gallagher, P.T., Williams, D.R., Mathioudakis, M., Phillips, K.J.H., & Keenan, F.P. 2002, ApJ, 567, L165,

12. Torrence, C. & G. P. Compo, 1998, A Practical Guide to Wavelet Analysis, Bull. Amer. Meteor. Soc., 79, 61

13. M^{c}Ateer, R.T.J., Gallagher, P.T., Williams, D.R., Mathioudakis, M., Phillips, K.J.H., & Keenan, F.P. 2002, ApJ, submitted

14. Baudin, F., Bocchialini, K., & Koutchmy, S. 1996, A&A, 314, L9